Chitosan-pectin hybrid nanoparticles prepared by coating and blending techniques

*Graphical Abstract (for review)

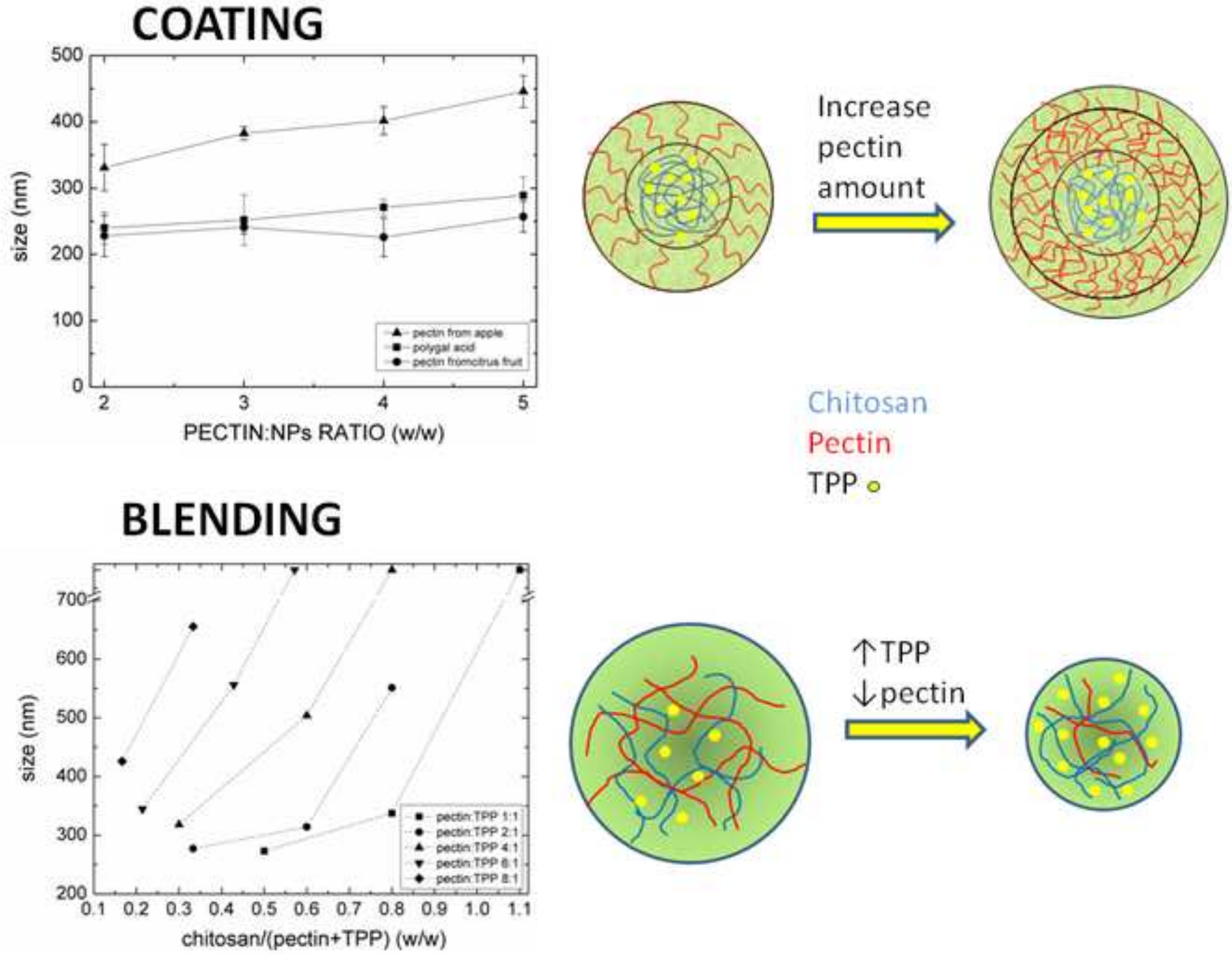

Chitosan-pectin hybrid nanoparticles prepared by coating and blending techniques

Rampino A[1§], Borgogna M[1], Bellich B[2,*], Blasi P[3,§,*], Virgilio F[1,4], Cesàro A[2,4].

Affiliations:

1 Dept. of Life Sciences, University of Trieste, Via Giorgieri 5, 34127 Trieste, Italy

[2] Dept. of Chemical and Pharmaceutical Sciences, University of Trieste, Via Giorgieri 1, 34127 Trieste, Italy

[3] Dept. of Chemistry and Technology of Drugs, University of Perugia, Via del Liceo 1, 06123 Perugia, Italy

[4] Elettra-Sincrotrone Trieste, Strada Statale 14 km 163.5, Area Science Park, 34149 Trieste, Italy

§ Present addresses: A.R. Laboratorio Nazionale-Consorzio Interuniversitario Biotecnologie (LNCIB), Area Science Park, Padriciano 99, 34149 Trieste, Italy; P.B. School of Pharmacy, Via S. Agostino n.1, University of Camerino, 62032 Camerino (MC)

*Corresponding author: Barbara Bellich
e-mail address: bbellich@units.it
Tel.: +39 0405588742;
Fax.: +39 0405583903

*Corresponding author: Paolo Blasi
e-mail address: paolo.blasi@unicam.it
Tel.: +39 737402289;
Fax: +39 737637345

ABSTRACT

The preparation of chitosan nanoparticles in combination with pectins, as additional mucoadhesive biopolymers, was investigated. Pectin from apple and from citrus fruit were considered; polygalacturonic acid was taken as a reference. Tripolyphosphate was used as an anionic cross-linker. Two different techniques were compared, namely the coating and the blending. Coated nanoparticles (NPs) in the ratio pectin:NPs from 2:1 to 5:1 evidenced that the size of NPs increased as the amount of pectin (both from apple and citrus fruit) was increased. In particular, for NPs coated with pectin from citrus fruit the size ranges from 200 to 260 nm; while for NPs coated with pectin from apple the size ranges from 330 to 450 nm. A minimum value of Z-potential around -35 mV was obtained for the ratio pectin:NPs 4:1, while further addition of pectin did not decrease the Z-potential. Also blended NPs showed a dependence of the size on the ratio of the components: for a given ratio pectin:tripolyphosphate the size increases as the fraction of chitosan increases; for a low ratio chitosan:pectin a high amount of tripolyphosphate was needed to obtain a compact structure. The effect of the additional presence of loaded proteins in chitosan-pectin nanoparticles was also investigated, since proteins contribute to alter the electrostatic interactions among charged species. FT-IR and DSC characterization are presented to confirm the interactions between biopolymers. Finally, the biocompatibility of the used materials was assessed by the chorioallantoic membrane assay, confirming the safety of the materials.

Keywords: Chitosan; pectin; hybrid nanoparticles; ionotropic gelation; coating and blending technique.

1. INTRODUCTION

Microspheres and microcapsules based on chitosan were developed for pharmaceutical applications and the importance of mucoadhesive properties for site specific drug delivery were described (He et al., 1998). The great potentiality of the use of chitosan as drug carrier is amply recognized. Various techniques have been described in literature for the preparation of chitosan microcarriers, as well as the parameters affecting drug release (Sinha et al., 2004). Different forms of chitosan based nanomaterials have been also reported in recent reviews (Borgogna et al., 2011; Shukla et al., 2012). The nanotechnological approach for the development of nanoparticle-based drug delivery systems has gained increase attention in the recent years (Desai, 2012). Several examples are reported in literature on the use of chitosan nanoparticles. More recently, rivastigmine loaded chitosan nanoparticles were investigated for intranasal delivery in case of Alzheimer's disease (Fazil et al., 2012); verapamil HCl loaded chitosan microspheres were studied for intranasal administration (Abdel Mouez et al., 2014); gemcitabine loaded in chitosan NPs was studied for oral delivery by Derakhshandeh and Fathi (2012).

One of the widely used techniques for the preparation of chitosan nanoparticles (NPs) is the ionic gelation, which is relatively simple and mild; it allows the successful encapsulation of labile molecules, such as proteins, since it avoids the use of organic solvents and high temperatures (Al-Qadi et al., 2012; Berger et al., 2004; Nasti et al., 2009; Xu and Du, 2003). The preparation of chitosan NPs following the method described by Calvo et al. (1997), was recently investigated focusing the attention on the effect of the ratio between chitosan and TPP (tripolyphosphate) on the loading of protein, being all charged species (Rampino et al., 2013). This study and other literature results (Papadimitiou et al., 2008; Bagre et al., 2013) show that small nanoparticles are obtained with a ratio of chitosan to TPP of 5:1. Moreover, chitosan is widely used for the preparation of several carriers due to its bioadhesive properties, its film forming abilities and low toxicity as well as its abundance in nature. Chitosan can interact with the constituents of the mucosal glycoprotein layer thus prolonging the residence time at the absorption site, increasing drug bioavailability (Sogias et al., 2012). The basic mechanisms of mucoadhesion have been reported and extensively commented (Andrews et al., 2009; Serra et al., 2009).

Pectin is another natural polysaccharide of pharmaceutical interest, whose properties mainly depend on the esterification degree. Its increasing use in the pharmaceutical field is due to its high availability in nature, its low or non toxicity nature and above all its mucoadhesive properties together with resistance to degradation by proteases and amylases. Such features make pectin attractive for the formulation of drug delivery carriers for many administration routes (Marras-

Marquez et al., 2015). In particular, the correlation between the mucoadhesive properties and the degree of methoxylation of different types of pectin has been investigated by Hagesaether et al. (2008). The same authors paid attention also to investigate the effect of formulation, i.e., when specific ions are added to the pectin solution. Indeed, on one side cross-linking can reduce the polymer mobility, therefore hampering its diffusion and interpenetration within mucin molecules; on the other side, particles of very small sizes have better potential to penetrate the mucus layer. In general, optimal size characteristics are required in order to achieve mucoadhesion by mean of the increased residence time and closer contact with mucosa. The possibility of obtaining hybrid nanoparticles, containing not only chitosan and TPP, but also other poly- or oligo-saccharides has been described in literature. Such hybrid systems are characterized by improved physical properties and better performances when used as drug delivery carriers (Goycoolea et al., 2009 and references therein).

The aim of this work was the investigation of two techniques, named coating and blending, for the preparation of hybrid pectin-chitosan nanoparticles.

Characterization of PEC properties in terms of size, charge, and surface morphology, shows the strict dependence on the macromolecular parameters of the polyions used (in addition to concentration, ionic strength, pH) and on the operative mixing conditions (interaction under resting or streaming mixing). For linear polymers the charge density (number of charges per unit length) defines not only the value for counterion condensation, but also the conditions for chain pairing. These comments may help the understanding of pectin-chitosan interaction with the co-presence of TPP, under the hypothesis of thermodynamic equilibrium. The practical effects of addition of pectin are investigated following the coating technique (post-synthesis of NPs) or the blending technique (during synthesis of NPs).

On one side the coating technique allows to create a core consisting of a polymer and a protein, thus ideally the protein is more protected from the outside environment due to the presence of an outer shell obtained by subsequent coating with a polymer. This is not presumably obtained by a blending technique where the protein is dispersed throughout the polymeric matrix. On the other side one of the main advantages of the blending technique is the possibility of the one-step formulation, that is not possible with the coating technique.

Thus, it has been possible to exploit the well known capability of chitosan to form nanoparticles, to obtain a drug delivery system based on the combination of two classes of mucoadhesive biopolymers.

2. MATERIALS AND METHODS

2.1 MATERIALS

Low molecular weight (LMW) chitosan (MW 150 kDa; [η] = 2.37 dL/g; degree of acetylation DA = 13%), polygalacturonic acid from orange, MW 18 kDa, degree of esterification (DE) 10,6% (Cesàro et al., 1982), pectin from citrus fruit (MW 17 kDa, DE 22%), pectin from apple (MW 30-100 kDa, degree of esterification 71%), bovine serum albumin (BSA), albumin from chicken egg albumen (OVA), technical grade pentasodium tripolyphosphate (TPP), sodium acetate, sodium hydroxide, and sodium chloride were all purchased from Sigma-Aldrich Co. (St. Louis, Missouri, USA). Acetic acid and hydrochloric acid were obtained from Carlo Erba Reagents (Carlo Erba, Milan, Italy). All other chemicals were of the highest purity grade commercially available and used without further purification.

The commercial chitosan sample was purified and characterized as reported elsewhere (Donati et al., 2005). The intrinsic viscosity of chitosan was measured by employing a Schott–Geräte AVS/G automatic apparatus and an Ubbelohde type viscometer (in acetate buffer 0.25 M, pH 4.7), as reported in the previous paper (Rampino et al., 2013).

2.2 METHODS

2.2.1 Nanoparticles preparation

Chitosan nanoparticles (NPs) were prepared using the ionotropic gelation method (Calvo et al., 1997; Rampino et al., 2013). A 0.25% w/v chitosan solution was prepared by dissolving LMW chitosan in 0.05% v/v acetic acid solution for 24 hours under stirring. The pH of the solution was adjusted to 5.5 with a sodium hydroxide solution while deionized water was added to obtain the desired final concentration. TPP was dissolved in deionized water at a concentration of 0.25% (w/v) and subsequently diluted to obtain solutions at different concentrations.

The TPP and chitosan solutions were filtered through a 0.45 µm mixed cellulose esters membrane (Millipore, Massachusetts, USA) to remove any insoluble matter. TPP solution was added drop wise to the chitosan solution under magnetic stirring at room temperature (Rampino et al., 2013).

Chitosan NPs have been loaded with two different model proteins: BSA and OVA, whose isoelectric points are 4.8 and 4.7, respectively. The protein were dissolved in deionized water (concentration 4 mg/mL) and added directly to the chitosan solution under magnetic stirring. Batches with different theoretical loading were prepared by adding different volumes of the protein stock solution, to obtain final protein concentrations of 200, 400, and 600 µg/mL. The solution,

containing chitosan and protein, was then diluted to a final volume of 5 mL using deionized water. After dropping the TPP solution, the dispersion was left under constant stirring for 30 min at room temperature. The suspension was centrifuged for 2 hours at 3270 RCF to remove the excess of chitosan and protein. The supernatant was collected separately while the sedimented particles were re-dispersed in deionized water, analyzed for their size and surface charge and then lyophilized.

2.2.2 Pectin-chitosan nanoparticles

Each pectin sample was dissolved in deionized water adjusting the pH between 6 and 7, thus forming the sodium salt. Hybrid pectin-chitosan NPs were prepared following two different procedures named coating (Borges et al., 2005) and blending (Alonso et al., 2006).

Coating

LMW Chitosan NPs suspension was added to a pectin solution drop wise at different ratios under magnetic stirring at room temperature. The suspension of coated particles was centrifuged for 2 h at 3270 RCF and the supernatant was discarded. Particles were re-dispersed in deionized water, characterized and freeze dried. Protein loaded NPs were prepared according to the procedure reported for sole chitosan NPs (Rampino et al., 2013). Pectin-coated NPs were prepared by using sodium polygalacturonate, pectin from citrus fruit and pectin from apple.

Blending

Chitosan and TPP solutions were prepared as previously described. TPP solution was mixed under magnetic stirring to pectin solution at different volume ratios. NPs formed spontaneously upon drop wise addition of the cationic solution to the anionic one under stirring. NPs were isolated by centrifuging at 3270 RCF for 2 h, the supernatant was discarded and the pellet re-dispersed in deionized water, characterized and freeze dried. Loaded NPs were prepared dissolving the model protein directly in the anionic solution containing TPP and pectin, and then the particles were prepared as previously described. Blended NPs were prepared by using pectin from apple.

2.2.3 Nanoparticle characterization: size and zeta potential

The size of the NPs and the surface zeta potential were determined using a Malvern Zetasizer Nano ZS (Malvern Instruments, Worcestershire, UK). Measurements were carried out at 25 °C in replicate of three.

2.2.4 Determination of protein loading efficiency

Six BSA and OVA standard solutions at different concentrations were prepared using a known amount of protein and analyzed with a bicinchoninic acid protein assay kit (BCA™) Sigma-Aldrich Co. (St. Louis, Missouri, USA) to build a calibration curve. 25 μL of each standard and sample were placed into a 96-well microplate and 200 μL of reagent was added. Each analysis was performed in a replicate of three. The microplate was incubated at 37 ^{o}C for 30 minutes after being thoroughly mixed for 30 seconds by a microplate shaker. The microplate was then cooled to room temperature, and the absorbance measured on a plate reader (Pierce, Illinois, USA). Spectrophotometric measurements were carried out at 562 nm, which does not overlap with polymer spectra. Unloaded NPs were used as control.

The amount of protein loaded in NPs was calculated as the difference between the protein total amount and the protein recovered in the supernatant after centrifugation, assuming that the amount not found in the supernatant was encapsulated in the NPs.

The loading efficiency experiments were carried out on native NPs containing chitosan:TPP 5:1 w/w, NPs coated with pectin from apple in the ratio from 2:1 to 5:1, loaded with BSA. Pectin from apple was used in blended NPs with a pectin:TPP ratio 4:1 w/w and a ratio between chitosan and the anionic components (pectin, TPP and protein) of 1.2:1 and 2:1, loaded with OVA.

2.2.5 Fourier transform-infrared (FT-IR) spectroscopy

IR spectra were recorded on lyophilized samples using a Vertex 70 (Bruker Optics GmbH) spectrophotometer (spectral resolution of 4 cm^{-1}) equipped with a MIRacle™ ATR devices (Pike Optics) with a single reflection diamond crystal (1.8 mm spot size) and using a MCT detector (HgCdTe, mercury-cadmium-tellurium) cooled with liquid nitrogen.

Samples of the raw materials and freeze dried NPs were placed on the top of the diamond crystal and stopped with a high-pressure clamp. Spectra were recorded in the range 5000-600 cm^{-1}.

FT-IR investigations were carried out on starting materials, chitosan:TPP NPs, coated NPs with pectin from apple and citrus fruit, blended NPs with pectin from apple.

2.2.6 Differential Scanning Calorimetry (DSC)

DSC analysis of raw materials, freeze dried uncoated, coated and blended pectin-chitosan NPs was carried out by using a PerkinElmer® DSC 6 calorimeter (PerkinElmer, Massachusetts, USA). Samples (about 2 mg) were accurately weighed into open aluminum pan and heated from 20 °C to 350 °C at a scanning rate of 10 °C/min under a nitrogen flow of 20 mL/min.

DSC investigations were carried out on on starting materials, chitosan:TPP NPs, coated NPs with pectin from apple and citrus fruit, blended NPs with pectin from apple.

2.2.7 Chorioallantoic membrane assay

The safety of raw materials (chitosan and pectin from apple), chitosan NPs and chitosan NPs coated with pectin from apple in the ratio pectin:NPs 2:1 w/w was evaluated *in vivo* by using the chick embryo chorioallantoic membrane (CAM) assay (Saw et al., 2008; Schoubben et al., 2013). Fertilized eggs were disinfected with alcohol 70° and placed in an incubator at 38 °C with 60% relative humidity. At incubation day 3, a window opening was punctured at the blunt end of the egg and living embryos were selected for the experiment. The opening was then covered with a polyethylene film glued with albumen to avoid water loss and microbial contamination. At incubation day 6, solid samples (6 mm tablet) were applied directly on the CAM. A Leica WILD M32 stereomicroscope (equipped with a WILD PLAN 1X lens), connected to a Leica DFC 320 camera system, was used to follow the evolution of any effect on the materials on the CAM. After 24 hours, all the eggs were examined again and all the acquired images were compared with those at time 0 and with the controls for qualitative acute toxicity evolution (Vargas et al., 2007).

3. RESULTS AND DISCUSSION

3.1. Chitosan and pectin samples used in nanoparticle preparation.

LMW chitosan NPs, produced following a previous optimized methodology, had a mean size and surface charge of 200 ± 24 nm and 25 ± 3 mV, respectively (Rampino et al., 2013). The production of hybrid pectin-chitosan NPs as drug delivery systems was investigated in view of the well-known mucoadhesive properties of pectins. The pectin samples were characterized by different values of molecular weight and degree of esterification (MW and DE, respectively): polygalacturonic acid (18 kDa and 10.6%), pectin from citrus fruit (17 kDa and 22%), pectin from apple (30-100 kDa and 71%). These macromolecular properties of the pectins and of chitosan sample used (MW 140 kDa and DE 13%) in addition to the coating or blending procedure used, govern and control the final characteristics of the hybrid NPs that can be effectively defined as poly-electrolyte complexes (PEC).

3.2. Pectin-chitosan nanoparticle preparation and characterization

3.2.1. Coating technique

Chitosan NPs, obtained using a chitosan:TPP ratio of 5:1 w/w, were centrifuged, re-dispersed and added to the pectin solution. Since chitosan NPs are characterized by a net positive surface charge and pectin is negatively charged at the pH (6-7) employed for the coating, the electrostatic interaction between opposite charges favors the complexation of pectin on the NPs outer surface. This is seen by the dependence of NPs size and Z-potential on the degree of esterification, molecular weight and concentration of the pectin used, as reported in **Fig. 1**.

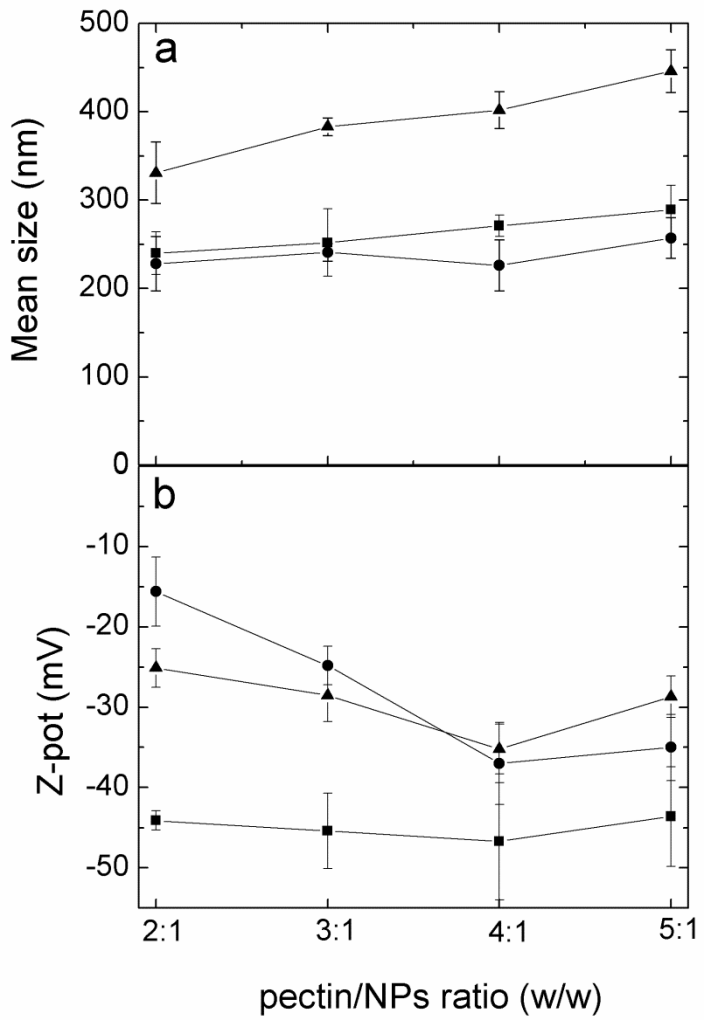

Fig. 1: mean size (a) and Z-potential (b) of chitosan NPs (chitosan:TPP ratio 5:1 w/w) coated with sodium polygalacturonate (■), pectin from citrus fruit (●) and pectin from apple (▲).

In all cases, an increase of the mean size is observed and, supposing that pectin is confined in the outer layer (coating), the thickness of the coating depended on the type and amount of pectin used. A remarkable size increase was recorded when apple pectin was used to coat chitosan NPs (**Fig. 1a)**, while a smaller increase in NPs size is produced with sodium polygalacturonate or citrus pectin. The behavior of apple pectin coating is clearly due to its higher MW and higher DE as compared with the other two pectin samples that show similar behavior due to the quite similar values of molecular weight and charge density of the two macromolecules.

As a further general comment, the larger the amount of pectin, the higher was the increase in particle size. However, this effect is particularly evident for the apple pectin, since the presence of a higher amount of low-charged polymer increases the coating thickness. As a speculative

observation (to be confirmed with the other results here reported), a more swollen coating would occur with apple pectin that has the highest DE.

As the pectin concentration is concerned, at pectin:NPs ratio less than 2:1, both apple and citrus pectins led to the formation of aggregates (data not shown), probably because of the low surface charge. Indeed, upon increasing pectin concentration the surface charge of NPs changes from positive to slightly negative producing particles with a Z-potential of -6 mV (data not shown), while for NPs stability a high charged surface is required to avoid their aggregation. It has been shown that such a low absolute value of Z-potential does not produce an efficient electrostatic repulsion between NPs leading to aggregation (Gonzalez-Mira et al., 2010).

Fig. 1b reports the NPs surface charge as a function of the pectin:NP ratio. At low pectin concentration (2:1) the value of Z-potential is very negative for sodium polygalacturonate (*ca* -45 mV), while for citrus pectin and for apple pectin is about -25 and -15 mV, respectively. Upon increasing pectin concentration, no changes in Z-potential are observed with sodium polygalacturonate, while both apple and citrus pectins reached a minimum value of about -35 mV at pectin:NPs ratio of 4:1 **(Fig. 1b)**. These findings suggest that an optimal level of coating (as derived from the value of Z-potential due to polymers complexation) can be identified and that a further addition of pectin to NPs only produces an increase in size.

3.2.2. Blending technique

The preparation of NPs by blending technique implies that chitosan is added to the anionic solution of pectin containing TPP, with the important advantage of a one-step procedure. The effect of the amount of pectin on NPs size has been investigated both as a function of the mass ratio between the cationic (chitosan) and anionic (pectin+TPP) components, and as a function of the ratio between pectin and TPP (**Fig. 2**).

For a given ratio between pectin and TPP, it was generally observed a size increase as the mass fraction of chitosan increased. A remarkable size increase was observed when a high amount of pectin was used and the ratio between pectin and TPP was high. A concomitant reduction of chitosan and pectin and an increase of TPP amount provoked a reduction of particle size. This might be due to the strong effect of TPP that produced a compact structure with chitosan that interacts with pectin. Thus, the dependence of the complexation stoichiometry on the reaction of the [$-COO^-$] and [$-NH_3^+$] functional groups of both polyelectrolytes was established, expressed as the ratio of the chitosan concentration in the NPs relative to the total pectin concentration.

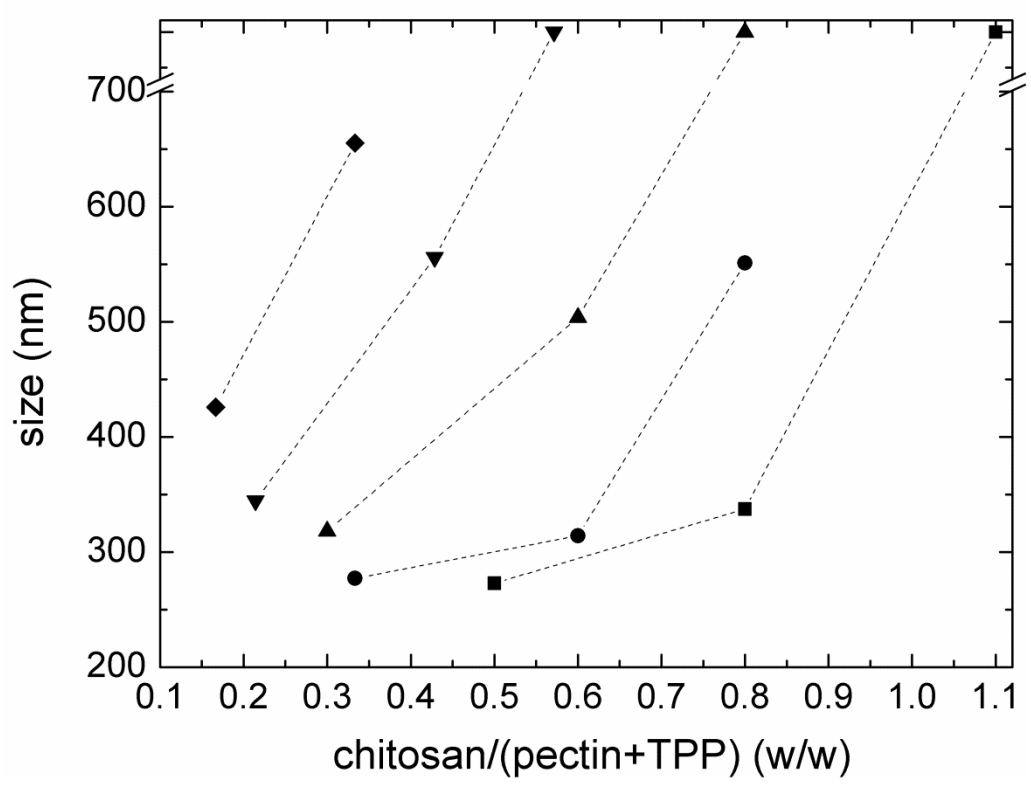

Fig. 2: mean size of chitosan NPs blended with apple pectin in different ratios with TPP. Ratio pectin:TPP 1:1 (■), 2:1 (●), 4:1 (▲), 6:1 (▼) and 8:1 (♦). The mean size of NPs in the absence of pectin is in the range of 200 nm.

For the same chitosan mass fraction, NPs with different size can be obtained depending on the ratio between pectin and TPP. A low mean size of NPs was obtained for formulations with a low pectin:TPP ratio. This is not surprising since a high concentration of TPP, available for ionic complexation, produces a highly compact polyelectrolytes network. When the concentration of pectin increased, the electrostatic interactions with less accessible $-NH3^{+}$ groups resulted in the formation of more swollen structures; this is due to the increase in the promotion of un-complexed stretches of the pectin chains. A trend for NPs size can be recognized suggesting that the lowest size of NPs (less than 300 nm) is obtained for chitosan mass fractions in the range between 0.3 and 0.5, and with pectin:TPP ratio 1:1 to 4:1.

A general decrease of the Z-potential was found as the amount of pectin was increased reaching values between -20 and -29 mV. For the same fraction of chitosan, NPs with different surface charge can be obtained depending on the ratio between pectin and TPP. For a given ratio, the lowest

surface charge is obtained with the highest ratio pectin to TPP. This aspect is particularly important in view of modulating NP surface properties.

As mentioned, the blending technique is preferred from the operational point of view since tedious steps, such as centrifugation and re-dispersion, are not necessary. In addition, the blending technique resulted suitable to prepare NPs even at chitosan:TPP ratio lower than 5:1 w/w, while this was not possible using the coating technique because of aggregation.

3.3 Effect of protein loading

The effect of two model proteins, BSA and OVA, was investigated since the addition of proteins to the formulation, either blending or coating, can further modify the equilibria established among chitosan, pectin and TPP, in relation to the charged groups on the protein surface (Yu et al., 2009). OVA and BSA are medium size globular protein with a molar mass of 45 and 66.5 kDa, respectively, a similar isoelectric point (4.9 and 4.7) and equal absolute negative charge of about -11*e* at pH 7. Therefore, the only difference would reside in the dimensions, being OVA 2/3 smaller that BSA (Stokes radius 3.1 and 3.5, respectively).

The loading efficiency of experiments were carried out on native NPs containing chitosan:TPP 5:1 w/w and NPs coated with pectin from apple in the ratio from 2:1 to 5:1. With the coating technique, the loading efficiency for BSA was similar to that found for uncoated NPs (chitosan:TPP 5:1 w/w), and ranging between 40% and 60% (Rampino et al. 2013), suggesting that the final step of coating did not induce protein loss. Furthermore, while the presence of protein did not significantly increase the size of the NPs, however, a relevant increase of the dimensions was detected after the coating with pectin. A direct correlation was found with the amount of pectin added, loaded NP mean diameter ranging from 700 nm to 1250 nm for ratio of pectin to NPs from 2:1 to 5:1 w/w. Given the pI of OVA and BSA (both slightly negative charged), an electrostatic interaction occurs between the positively charged chitosan and the negatively charged proteins, therefore screening chitosan for further interaction with pectin and producing much less compact polymer particles. Loaded NPs were characterized by Z-potential values slightly lower than unloaded NPs. In addition, the decrease of the Z-potential was as pronounced as the loading increased. The subsequent addition of pectin completely changes the surface charge from positive to negative. The Z-potential was around -38 mV, sufficient to maintain a permanent electrostatic repulsion and avoid the aggregation.

Pectin from apple was used in blended NPs with a pectin:TPP ratio 4:1 w/w and a ratio between chitosan and the anionic components (pectin, TPP and protein) of 1.2:1 and 2:1. Regarding the

blending technique, experiments with OVA suggested a possible competition between pectin and ovalbumin. Indeed, the loading efficiency, ranging between 16% and 27%, was lower than the corresponding unblended; pure chitosan NPs had a loading efficiency between 48% and 76% (Rampino et al. 2013), depending on the initial amount. A decrease of the loading efficiency was found as the amount of pectin increased and minor effects were observed on NPs size (an increase of about 50 nm was observed), while the value of Z-potential was similar to that of unblended NPs.

3.4 FTIR-ATR spectroscopic evidence for polymer interaction

FT-IR investigations were carried out coated NPs with pectin from apple and citrus fruit and blended NPs with pectin from apple; for comparison starting materials and native chitosan:TPP NPs are also reported. The solid state studies (FT-IR and DSC) have been conducted on empty NPs. The presence of a protein would have added another variable for the experiments. Chitosan spectrum shows a broad absorption between 3350 and 3270 cm^{-1} (**Fig. 3a**) previously attributed to a combination of stretching modes of O-H and N-H bonds in chitosan and to hydrogen bonds among polysaccharide chains. **Fig. 3a** shows that the same band becomes broader and shifted to lower wavenumbers in the sample of chitosan NPs, thus indicating an enhancement of the hydrogen bonds system (Mishra et al., 2008). The main peaks recognized for the chitosan sample were related to C=O stretching amide I at 1635 cm^{-1} and to amide II at 1539 cm^{-1} (Woranuch and Yoksan, 2013). These peaks slightly shifted to 1633 cm^{-1} and to 1543 cm^{-1} in the chitosan NPs sample, with an increase of intensity for the latter. The presence of this intense band at 1543 cm^{-1} is attributed to the bond formation between the amino groups of chitosan and TPP (Azevedo et al., 2011). Similar considerations were done by Xu and Du (2003) studying chitosan film treated with NaH_2PO_4 (Knaul et al., 1999). Other characteristic bands of chitosan NPs are the peak at 1213 cm^{-1} attributed to the P=O of the TPP, the intense band around 1070 cm^{-1} corresponding to C-O stretching and the pyranose ring at 890 cm^{-1} (Woranuch and Yoksan, 2013).

Fig. 3b-d reports the FTIR spectra of chitosan NPs coated with the three different pectin considered (sodium polygalacturonate, apple pectin and citrus fruit pectin) or blended with apple pectin. The spectra are reported in the range between 600 cm^{-1} and 1800 cm^{-1}, since major changes occur within this range. The region 1000 – 1200 cm^{-1} contains skeletal C-O and C-C vibration bands of glycosidic bonds and pyranose ring (Synytsya et al., 2003).

388 The main changes were in the region 1500-1700 cm^{-1} corresponding to the stretching vibrations of
389 amide bond and indeed the interaction of chitosan with pectin involves amine groups on chitosan
390 (not yet involved in bonds with TPP) and carboxylic groups of pectin (**Fig. 3b**).
391 Polygalacturonate shows only one peak around 1608 cm^{-1}; the two characteristic peaks of chitosan
392 NPs disappeared giving only one peak at 1593 cm^{-1} with a small shoulder after the coating with
393 polygalacturonate. A peak at 1410 cm^{-1} was identified and attributed to C-OH stretching of the
394 carboxylic group (Synytsya et al., 2003), as similarly observed for alginate (Sarmento et al., 2006a).
395 Apple pectin and citrus fruit pectin (**Fig. 3c-3d**) are characterized by the C=O stretching at 1608
396 and 1600 cm^{-1} respectively and by an additional peak, respectively at 1741 and 1743 cm^{-1},
397 corresponding to the C=O stretching in the ester form (Synytsya et al., 2003). In the apple pectin
398 sample the two peaks of C=O stretching have comparable intensity, due to the high degree of
399 esterification. As similarly observed for the polygalacturonate, the coating with apple pectin and
400 citrus fruit pectin gives rise to a single peak, respectively at 1597 and 1591 cm^{-1}, due to the
401 presence of the pectin on the surface on the NPs, and a small shoulder, in both cases at 1535 cm^{-1},
402 as already commented for the chitosan NPs formation. The peak around 1400 cm^{-1}, that was a
403 double peak in the chitosan NPs, becomes a single peak and it is shifted to 1410 cm^{-1} after coating.
404 The peaks attributed to the stretching of C=O in the ester form are still visible, but less intense. The
405 shifts observed in the two pectins vary only slightly from one to another, probably suggesting that
406 the different degree of esterification does not affect the number of interactions that are formed with
407 amino groups of chitosan.

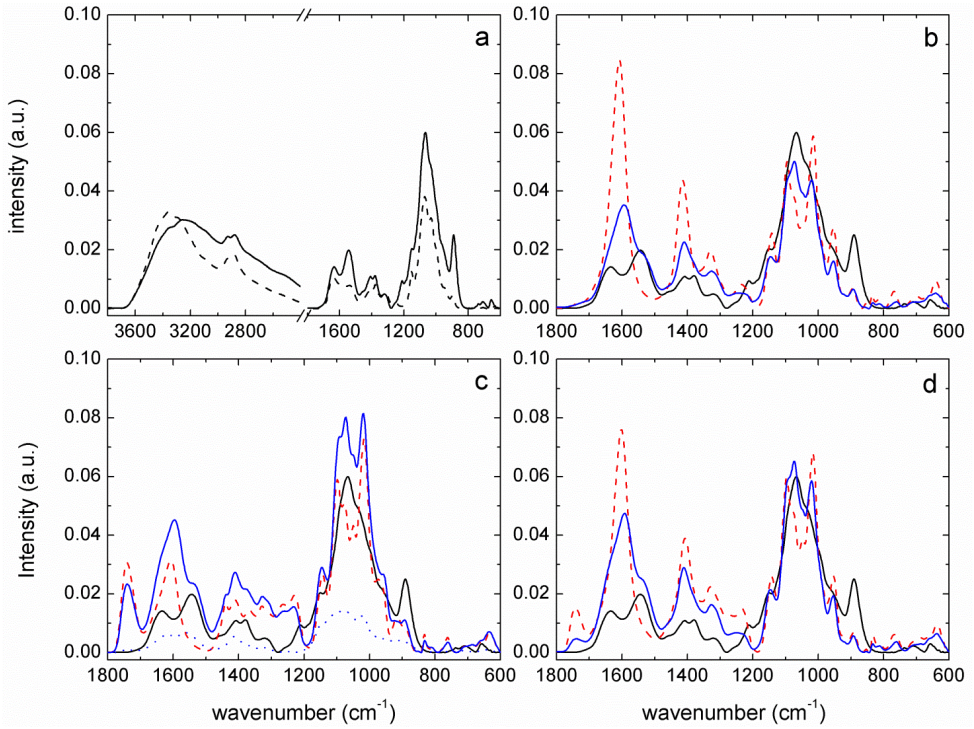

Fig. 3. FTIR spectra of a) chitosan (dash line) and chitosan NPs (full line); b) chitosan NPs (black full line), polygalacturonate (red dash line), polygalacturonate coated NPs (blue full line); c) chitosan NPs (black full line), apple pectin (red dash line), apple pectin coated NPs (blue full line) and apple pectin blended NPs (blue dot line); d) chitosan NPs (black full line), citrus fruit pectin (red dash line), citrus fruit pectin coated NPs (blue full line).

The effect of the shift is more pronounced for the sample coated with polygalacturonate. The important outcome is that the shift of these bands indicates a change in the environment of amino and carboxyl groups through the mutual interaction (Bigucci et al., 2008). From the presence of peaks different from those of the uncoated NPs it was possible to confirm the existence of a coating layer of pectin around the NPs, as also commented for alginate (Borges et al., 2005).

Fig. 3c reports the spectra of pectin-chitosan NPs obtained by blending technique. It has to be noticed that the bands are broader than that found for the corresponding coated NPs. A weak peak at 1741 cm^{-1} corresponding to the C=O stretching of the ester group of the pectin is still observed. The peak at 1608 cm^{-1} corresponding to the asymmetric stretching of carboxylate group shifts to 1597 cm^{-1} in case of the coated NPs; in case of the blended NPs it is still possible to identify the two peaks characterizing the chitosan NPs, at 1635 cm^{-1} and 1542 cm^{-1}, but these peaks are shifted of a few cm^{-1} (to 1616 cm^{-1} and to 1564 cm^{-1}) and are of comparable intensity.

The shift of the band at 1564 cm^{-1} (attributed to N-H bending) is greater than what has been observed in the coated samples. This could be due to the fact that the bending modes are sensitive to the changes in the environment of the group and so are more affected by a perturbative surrounding than the stretching modes. Therefore this shift of the N-H bending band could be indicative of a greater number of interaction between the amino groups of chitosan and the carboxyl groups of pectin, compared to the coated samples (Bigucci et al., 2008).

3.5 Differential scanning calorimetry

DSC investigations were carried out on coated NPs with pectin from apple and citrus fruit and on blended NPs with pectin from apple; for comparison starting materials and native chitosan:TPP NPs are also reported. DSC data of pure chitosan are characterised by an endothermal event (peak temp at 57.2 °C) corresponding to the dehydration and by an exothermal event that begins at 252 °C with a peak around 320 °C corresponding to the thermal degradation (Sarmento et al., 2006a; Sarmento et al., 2006b). In addition to the dehydration endothermic event (peak at 54.3 °C), chitosan NP DSC data revealed another endothermic event at 225 °C that has been ascribed to the breakdown of unspecific electrostatic interactions by Borges et al. (2005). The authors reported also a second endothermic peak of minor intensity, related to the cleavage of electrostatic interactions between chitosan and the counterion (sulphate ions in that case). In our case (TPP as counterion) a similar second peak was observed, and it is similarly attributed to the cleavage of such interactions. Indeed, the thermogram of TPP alone evidenced an endothermic peak at 192 °C; therefore, it could also derive from the TPP, although shifted to higher temperatures in NPs. The exothermic event beginning at 243.8 °C with a peak around 310 °C, and corresponding to thermal degradation, is slightly shifted to lower temperatures (Bagre et al., 2013) as a result of the interaction of chitosan with TPP (Azevedo et al., 2011). The intensity of the exothermal event for chitosan NPs is lower than that of the native chitosan (similar weight are compared); this is reasonably due to the fact that a fraction of the chitosan chain is cross-linked with TPP and therefore differently susceptible to degradation.

Pectin from apple is characterized by the endothermal event corresponding to dehydration and by two sharp exothermal peaks at 255 °C and 328 °C, corresponding to degradation **(Fig. 4b)**. Apart from the endothermal event of dehydration, chitosan NPs coated with apple pectin are characterized by an exothermal event starting at 273 °C with a peak at 324 °C, suggesting a thermal stabilization due to the interaction of chitosan with pectin and not only to TPP. The interaction is also confirmed

by the absence of any characteristic peaks of the pectin. The thermogram of pectin chitosan blended NPs did not reveal any characteristic peak of the apple pectin; the only difference observed was that the height of the exothermal event is far higher than that of the chitosan NPs and it is similar to chitosan alone, so not cross-linked with TPP. A lower interaction between chitosan and TPP, reasonably due to a competition between TPP and pectin, both negatively charged, would explain the recorded data.

Pectin from citrus fruit is characterized by an exothermal event between 225 and 250 °C with two distinct peaks at 232 and 248 °C, and another exothermal sharp peak at 331 °C **(Fig. 4c)**. The thermogram of chitosan NPs coated with citrus fruit pectin is characterized by an exothermic event with a peak at 318 °C, similar to that of NPs coated with apple pectin. As previously commented for apple pectin samples, characteristic peaks of the citrus fruit pectin were not found, confirming the interaction of pectin with chitosan as already evidenced by surface charge measurements.

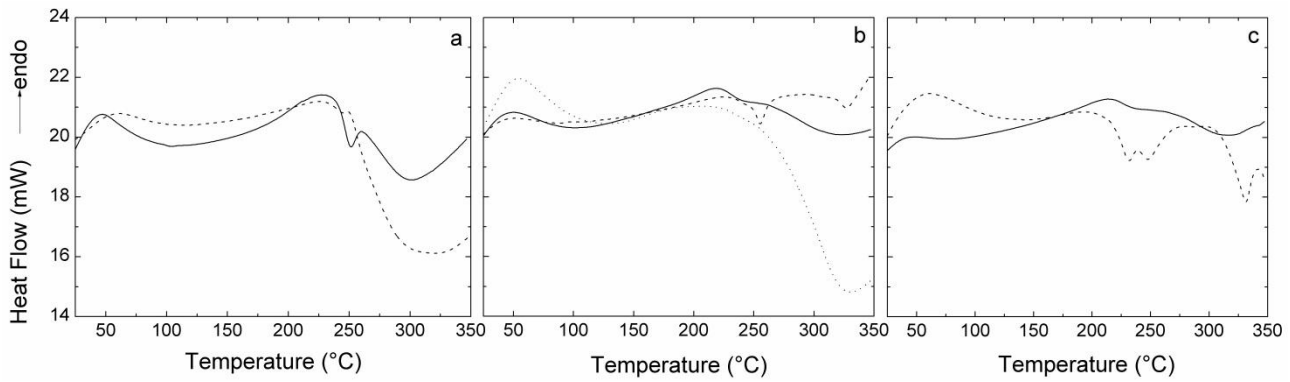

Fig. 4: DSC curves of a) chitosan (dash line) and chitosan NPs (straight line); b) apple pectin (dash line), coated NPs (straight line) with pectin and blended NPs (dot line) with pectin; c) citrus fruit pectin (dash line) and coated NPs (straight line) with pectin.

3.6 Chorioallontoic membrane assay (CAM)

CAM of 6 days old chicken embryos are shown in **Fig. 5a-d**. Because of eggs incubation in vertical position (convex pole in upper position), CAM floats over the yolk sack and, while growing, will cover all the air-exposed surface adhering to most of the testaceous membrane internal surface. Intrinsic CAM characteristics (e.g., high transparency, high vascularization and capillarity, sensitivity to physical and chemical insults) give this structure the right features for the direct and continuous evaluation of acute inflammatory response (Vargas et al., 2007; Saw et al., 2008).

The tested materials showed different behaviors in terms of dissolution/dispersion in the albumen wetting CAM surface. After deposition on CAM surface, pectin from apple swelled and polysaccharide chains rapidly disperse in the albumen film covering the membrane (**Fig. 5a' and 5a''**). The material was not visible 24 hours after deposition. On the contrary, 24 hours after deposition, chitosan, chitosan NPs, and chitosan-pectin NPs swelled generating transparent gels that did not disperse in the albumen film (**Fig. 5**). Transparency allowed to visualize easily the portion of CAM under the material and not just the space around the implant. A careful observation of treated embryos (1 day after treatment) evidences the complete absence of the signs ascribable to acute toxicity, inflammation or pro-angiogenic effect, and no substantial differences were evidenced between the raw materials and NPs (**Fig. 5**). The same results are obtained with saline, the negative control routinely employed in our laboratories in this experimental setup (Blasi et al., 2013) and confirmed here (**Fig. 5**). TPP, being ionically bound to chitosan amino groups, does not impair the biocompatibility of the NPs evaluated. TPP has shown to be extremely toxic with the same experimental setup (Rampino et al., 2013). Membrane opacity, bleeding, vessel rupture, CAM corrosion, capillary and vessel overgrowth, are the classical reactions to substances or materials provoking a toxic insult or an inflammation on this extraembryonic membrane. Additionally, a substance having pro- or anti-angiogenic effect is responsible of the increase or decrease of capillaries/vessels density under and/or around the treated zone. These effects are experienced by deposing aggressive surfactants, such as sodium dodecilsulphate (Blasi et al., 2013), or polysaccarides, such as λ carrageenan (**Fig. 5**), that are used as positive controls.

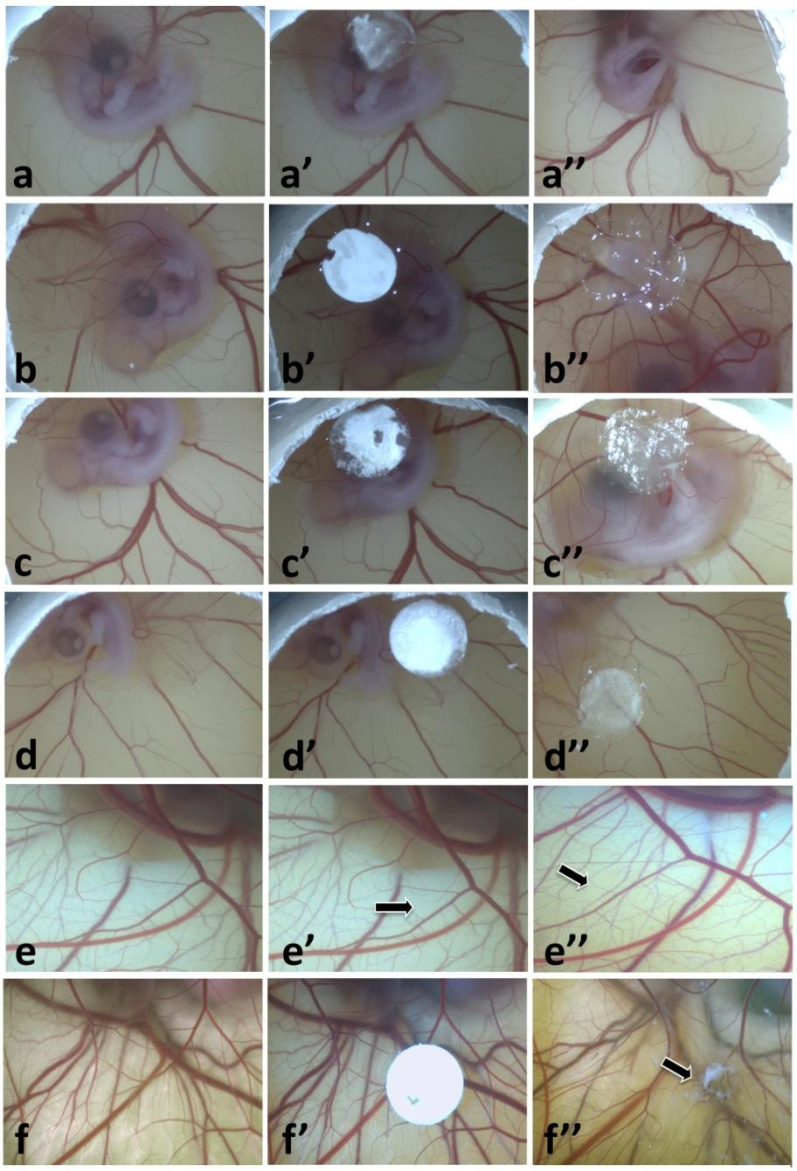

Fig. 5 Chicken embryos at different stages of development observed during acute toxicity experiments. a, embryo before treatment; a', after material (apple pectin) deposition; a" after 24 hours - b, embryo before treatment; b', after material (chitosan) deposition; b" after 24 hours - c, embryo before treatment; c', after material (chit/pect NPs) deposition; c" after 24 hours - d, embryo before treatment; d', after material (chit NPs) deposition; d" after 24 hours - e, embryo before treatment; e', after saline deposition (negative control); e" after 24 hours - f, embryo before treatment; f', after material (λ carrageenan) deposition (positive control); f" after 24 hours.

4. CONCLUSIONS

Chitosan in combination with pectins confirmed to be a valuable biopolymer for the preparation of carriers interesting for drug delivery applications, due to the possibility to tailor the physico-chemical characteristics of the final NPs.

The most relevant outcome is the large number of potentially useful nanoparticles prepared with the two procedures, which, however, has been a challenge for selecting a few batches for characterization and testing studies. A rationalization would imply that the actual composition of NPs and not simply the starting composition is taken as a characterizing parameter of the products. Unfortunately, to the best of our knowledge, this approach is not yet reported in literature. The results here presented evidenced that it was possible to prepare pectin:chitosan NPs with both techniques, as already reported for other polymers. Two main advantages resulted from the blending technique: the first is the one-step preparation, that is highly desirable especially in view of a scale-up process, the second one is the possibility to tune the size and Z-potential by properly selecting the ratio of chitosan, pectin and TPP. The coating technique did not allow such a modulation of size, since the addition of pectin as external NPs coating always increases the size. It is worth noticing that the addition of a protein requires to take into account the competition among charged species. Indeed, a decrease of the loading of BSA and OVA was found in case of the blending technique due to the electrostatic interactions of chitosan with protein and pectin, both negatively charged. This brings to the conclusion that the most suitable technique depends on the physico-chemical characteristics of the species involved, i.e. polymer and protein.

Acknowledgment

This work has been partially carried out within the European Project FP6 NanoBioPharmaceutics (NMP 026723-2). Antonio Rampino was the recipient of a grant from MIUR (Rome) during his Ph.D. studies on “Polysaccharide-based nanoparticles for drug delivery”. The Authors are indebted to Mr. Lanfranco Barberini for the precious support in chicken embryo chorioallantoic membrane assay.

553

554

References

Alonso-Sande, M., Cuña, M., Remuñán-López, C., Teijeiro-Osorio, D., Alonso-Lebrero, J.L., Alonso, M.J., 2006. Formation of new glucomannan-chitosan NPs and study of their ability to associate and deliver proteins. Macromolecules, 39, 4152-4158.

Al-Qadi, S., Grenha, A., Carrión-Recio, D., Seijo, B., Remuñán-López, C., 2012. Microencapsulated chitosan nanoparticles for pulmonary protein delivery: in vivo evaluation of insulin-loaded formulations. J. Control. Release 157, 383-390.

Andrews, G.P., Laverty, T.P., Jones, D.S., 2009. Mucoadhesive polymeric platforms for controlled drug delivery. Eur. J. Pharm. Biopharm. 71, 505-518.

Azevedo, J.R., Sizilio, R.H., Brito, M.B., Costa, A.M.B., Serafini, M.R., Araújo, A.A.S., Santos, M. R.V., Lira, A.A.M., Nunes, R.S., 2011. Physical and chemical characterization insulin-loaded chitosan-TPP nanoparticles. J. Therm. Anal. Calorim. 106, 685-689.

Bagre, A.P., Jain, K., Jain, N.K., 2013. Alginate coated chitosan core shell nanoparticles for oral delivery of enoxaparin: In vitro and in vivo assessment. Int. J. Pharm. 456, 31-40.

Berger, J., Reist, M., Mayer, J.M., Felt, O., Peppas, N.A., Gurny, R., 2004. Structure and interactions in covalently and ionically crosslinked chitosan hydrogels for biomedical applications. Eur. J. Pharm. Biopharm. 57, 19-34.

Bigucci, F., Luppi, B., Cerchiara, T., Sorrenti, M., Bettinetti, G., Rodriguez, L., Zecchi, V., 2008. Chitosan/pectin polyelectrolyte complexes: selection of suitable preparative conditions for colon-specific delivery of vancomycin. Eur. J. Pharm. Sci. 35, 435-441.

Blasi, P., Schoubben, A., Traina, G., Manfroni, G., Barberini, L., Alberti, P.F., Cirotto, C., Ricci, M., 2013. Lipid nanoparticles for brain targeting III. Long-term stability and in vivo toxicity. Int. J. Pharm. 454, 315-323.

Borges, O., Borchard G., Verhoef, J.C., Sousa, A., Junginger, H.E., 2005. Preparation of coated NPs for a new mucosal vaccine delivery systems. Int. J. Pharm., 229, 155-166.

Borgogna, M., Bellich, B., Cesàro, A., 2011. Marine Polysaccharides in Microencapsulation and Application to Aquaculture: "From Sea to Sea". Mar. Drugs 9, 2572-2604.

Calvo, P., Remunan-Lopez, R., Vila-Jato, C.J.L., Alonso, M.J., 1997. Chitosan and chitosan/ethylene oxide–propylene oxide block copolymer NPs as novel carriers for proteins and vaccines. Pharm. Res. 14, 1431-1436.

Cesàro, A., Ciana, A., Delben F., Manzini, G., Paoletti, S., 1982. Physicochemical properties of pectic acid. I. Thermodynamic evidence of a pH-induced conformational transition in aqueous solution. Biopolymers 21, 431-449.

Derakhshandeh, K., Fathi, S., 2012. Role of chitosan nanoparticles in the oral absorption of Gemcitabine. Int. J. Pharm. 437, 172-177.

591 Desai, N., 2012. Challenges in development of nanoparticle-based therapeutics. The AAPS journal,
592 14, 282-295.

593 Donati I., Stredanska, S., Silvestrini, G., Vetere, A., Marcon, P., Marsich, E., Mozetic, P., Gamini,
594 A., Paoletti, S., Vittur, F., 2005. The aggregation of pig articular chondrocyte and synthesis of
595 extracellular matrix by a lactose-modified chitosan. Biomaterials 26, 987-998.
596
597 Fazil, M., Md, S., Haque, S., Kumar, M., Baboota, S., Ali, J., 2012. Development and evaluation of
598 rivastigmine loaded chitosan nanoparticles for brain targeting. Eur. J. Pharm. Sci. 47, 6-15.

599 Gonzalez-Mira, E., Egea, M.A., Garcia, M.L., Souto, E.B., 2010. Design and ocular tolerance of
600 flurbiprofen loaded ultrasound-engineered NLC. Colloids Surf. B Biointerfaces 81, 412-421.

601 Goycoolea, F.M., Lollo, G., Remunan-Lopez, C., Quaglia, F., Alonso, M.J., 2009. Chitosan-
602 alginate blended nanoparticles as carriers for the transmucosal delivery of macromolecules.
603 Biomacromolecules 10, 1736-1743.

604 Hagesaether, E., Bye, R., Sande, S.A., 2008. Ex vivo mucoadhesion of different zinc-pectinate
605 hydrogel beads. Int. J. Pharm 347, 9-15.

606 He, P., Davis, S.S., Illum, L.,1998. In vitro evaluation of the mucoadhesive properties of chitosan
607 microspheres. Int. J. Pharm. 166, 75-68.

608 Knaul, J.Z., Hudson, S.M., Creber, K.A.M., 1999. Improved mechanical properties of chitosan
609 fibers. J. Appl. Polym. Sci. 72, 1721-1731.

610 Marras-Marquez, T., Peña, J., Veiga-Ochoa, M.D., 2015. Robust and versatile pectin-based drug
611 delivery systems. Int. J. Pharm 479, 265-276.

612 Mishra, R. K., Datt, M., Banthia, A. K., 2008. Synthesis and characterization of pectin/PVP
613 hydrogel membranes for drug delivery system. AAPS PharmSciTech 9, 395-403.

614 Mouez, A., Zaki, N. M., Mansour, S., Geneidi, A. S., 2014. Bioavailability enhancement of
615 verapamil HCl via intranasal chitosan microspheres. Eur. J. Pharm. Sci. 51, 59-66.

616 Nasti, A., Zaki, N.M., De Leonardis, P., Ungphaiboon, S., Sansongsak, P., Rimoli, M.G., Tirelli, N.,
617 2009. Chitosan/TPP and chitosan/TPP-hyaluronic acid nanoparticles: systematic optimisation of the
618 preparative process and preliminary biological evaluation. Pharm. Res. 26, 1918-1930.

619 Papadimitriou, S., Bikiaris, D., Avgoustakis, K., Karavas, E., Georgarakis, M., 2008. Chitosan
620 nanoparticles loaded with dorzolamide and pramipexole. Carbohydr. Polym. 73, 44-54.

621 Rampino, A., Borgogna, M., Blasi, P., Bellich, B., Cesàro, A., 2013. Chitosan NPs: Preparation,
622 size evolution and stability. Int. J. Pharm. 455, 219-228.

623 Sarmento, B., Ferreira, D., Veiga, F., Ribeiro, A., 2006a. Characterization of insulin-loaded alginate
624 nanoparticles produced by ionotropic pre-gelation through DSC and FTIR studies. Carbohydr.
625 Polym. 66, 1-7.

626 Sarmento, B., Martins, S., Ribeiro, A., Veiga, F., Neufeld, R., Ferreira, D., 2006b. Development
627 and comparison of different nanoparticulate polyelectrolyte complexes as insulin carriers. Int. J.
628 Pept. Res. Ther. 12, 131-138.

629 Saw, C.L.L., Heng, P.W.S., Liew, C.V., 2008. Chick chorioallantoic membrane as an in situ
630 biological membrane for pharmaceutical formulation development: a review. Drug Dev. Ind.
631 Pharm. 34, 1168-1177.

632 Schoubben, A., Blasi, P., Marenzoni, M.L., Barberini, L., Giovagnoli, S., Cirotto, C., Ricci,M.,
633 2013. Capreomycin supergenerics for pulmonary tuberculosis treatment:preparation, in vitro, and in
634 vivo characterization. Eur. J. Pharm. Biopharm. 83, 388-395.

635 Serra, L., Doménech, J., Peppas, N.A., 2009. Engineering design and molecular dynamics of
636 mucoadhesive drug delivery systems as targeting agents. Eur. J. Pharm. Biopharm. 71, 519-528.

637 Shukla, S.K., Mishra, A. K., Arotiba, O.A., Mamba, B.B., 2013. Chitosan-based nanomaterials: A
638 state-of-the-art review. Int. J. Biol. Macromol. 59, 46-58.

639 Sinha, V.R., Singla, A.K., Wadhawan, S., Kaushik, R., Kumria, R., Bansal, K., Dhawan, S., 2004.
640 Chitosan microspheres as a potential carrier for drugs. Int. J. Pharm. 274, 1-33.

641 Sogias, I.A., Williams, A.C., Khutoryanskiy, V.V., 2012. Chitosan-based mucoadhesive tablets for
642 oral delivery of ibuprofen. Int. J. Pharm. 436, 602-610.

643 Synytsya, A., Copìkova, J., Matejka, P., Machovic, V., 2003. Fourier transform Raman and infrared
644 spectroscopy of pectins. Carbohydr. Polym. 54, 97-106.

645 Vargas, A., Zeisser-Labouèbe, M., Lange, N., Gurny, R., Delie, F., 2007. The chickembryo and its
646 chorioallantoic membrane (CAM) for the in vivo evaluation of drug delivery systems. Adv. Drug
647 Deliv. Rev. 59, 1162-1176.

648 Woranuch, S., Yoksan, R., 2013. Eugenol-loaded chitosan nanoparticles: I. Thermal stability
649 improvement of eugenol through encapsulation. Carbohydr. Polym. 96, 578-585.

650 Xu, Y., Du, Y., 2003. Effect of molecular structure of chitosan on protein delivery properties of
651 chitosan nanoparticles. Int. J. Pharm. 250, 215-226.

652 Yu, C.Y., Yin, B.C., Zhang, W., Cheng, S.X., Zhang, X.Z., & Zhuo, R.X., 2009. Composite
653 microparticle drug delivery systems based on chitosan, alginate and pectin with improved pH-
654 sensitive drug release property. Colloids Surf. B Biointerfaces 68, 245-249.
655

656 **CAPTION TO FIGURES**:

657 **Fig. 1:** mean size (a) and Z-potential (b) of chitosan NPs (chitosan:TPP ratio 5:1 w/w) coated with
658 sodium polygalacturonate (■), pectin from citrus fruit (●) and pectin from apple (▲).
659

Fig. 2: mean size of chitosan NPs blended with apple pectin in different ratios with TPP. Ratio pectin:TPP 1:1 (■), 2:1 (●), 4:1 (▲), 6:1 (▼) and 8:1 (♦). The mean size of NPs in the absence of pectin is in the range of 200 nm.

Fig. 3: FTIR spectra of a) chitosan (dash line) and chitosan NPs (full line); b) chitosan NPs (black full line), polygalacturonate (red dash line), polygalacturonate coated NPs (blue full line); c) chitosan NPs (black full line), apple pectin (red dash line), apple pectin coated NPs (blue full line) and apple pectin blended NPs (blue dot line); d) chitosan NPs (black full line), citrus fruit pectin (red dash line), citrus fruit pectin coated NPs (blue full line).

Fig. 4: DSC curves of a) chitosan (dash line) and chitosan NPs (straight line); b) apple pectin (dash line), coated NPs (straight line) with pectin and blended NPs (dot line) with pectin; c) citrus fruit pectin (dash line) and coated NPs (straight line) with pectin.

Fig. 5: Chicken embryos at different stages of development observed during acute toxicity experiments. a, embryo before treatment; a', after material (apple pectin) deposition; a" after 24 hours - b, embryo before treatment; b', after material (chitosan) deposition; b" after 24 hours - c, embryo before treatment; c', after material (chit/pect NPs) deposition; c" after 24 hours - d, embryo before treatment; d', after material (chit NPs) deposition; d" after 24 hours - e, embryo before treatment; e', after saline deposition (negative control); e" after 24 hours - f, embryo before treatment; f', after material (λ carrageenan) deposition (positive control); f" after 24 hours.